Oregon State UNIVERSITY OSU

Seasonal hydrologic responses to climate change in the Pacific Northwest

Julie A. Vano[1,2], Bart Nijssen[1], and Dennis P. Lettenmaier[1,3]

[1]Department of Civil and Environmental Engineering, University of Washington, Seattle, Washington, USA, [2]Now at College of Earth, Ocean, and Atmospheric Sciences, Oregon State University, Corvallis, Oregon, USA, [3]Now at Department of Geography, University of California Los Angeles, Los Angeles, California, USA

Abstract Increased temperatures and changes in precipitation will result in fundamental changes in the seasonal distribution of streamflow in the Pacific Northwest and will have serious implications for water resources management. To better understand local impacts of regional climate change, we conducted model experiments to determine hydrologic sensitivities of annual, seasonal, and monthly runoff to imposed annual and seasonal changes in precipitation and temperature. We used the Variable Infiltration Capacity (VIC) land-surface hydrology model applied at 1/16° latitude-longitude spatial resolution over the Pacific Northwest (PNW), a scale sufficient to support analyses at the hydrologic unit code eight (HUC-8) basin level. These experiments resolve the spatial character of the sensitivity of future water supply to precipitation and temperature changes by identifying the seasons and locations where climate change will have the biggest impact on runoff. The PNW exhibited a diversity of responses, where transitional (intermediate elevation) watersheds experience the greatest seasonal shifts in runoff in response to cool season warming. We also developed a methodology that uses these hydrologic sensitivities as basin-specific transfer functions to estimate future changes in long-term mean monthly hydrographs directly from climate model output of precipitation and temperature. When principles of linearity and superposition apply, these transfer functions can provide feasible first-order estimates of the likely nature of future seasonal streamflow change without performing downscaling and detailed model simulations.

1. Introduction

The Pacific Northwest (PNW), defined as the Columbia River basin and its coastal drainages (Figure 1), has strong seasonal variations in runoff. This is due to the combined effects of a Mediterranean climate, in which most precipitation occurs in the fall and winter, and complex topography, wherein snow accumulates in winter and melts in spring and summer. The region's snowpack effectively serves as a natural reservoir that slowly releases water throughout the dry season providing sustained streamflow critical for agriculture, fisheries, and municipal and industrial use. Manmade reservoirs also serve this purpose, but can hold only ∼30% of the region's annual streamflow and depend on snowmelt for in-season resupply [*Federal Columbia River Power System* (*FCRPS*), 2001].

A number of authors have previously studied the impact of climate variations on streamflow in the PNW [e.g., *Hamlet and Lettenmaier*, 1999; *Payne et al.*, 2004; *Luce and Holden*, 2009; *Lee et al.*, 2009; *Elsner et al.*, 2010; *Hamlet et al.*, 2010; *Luce et al.*, 2013; *Safeeq et al.*, 2014]. The motivations for these studies stem from the region's vast hydropower resources [*Lee et al.*, 2009], dangers of flooding [*Payne et al.*, 2004], endangered species issues related to anadromous fish [*Mantua et al.*, 2010], agricultural water uses [*Vano et al.*, 2010], and the need to manage reservoir systems to balance these needs [*Hamlet*, 2011].

Many of these past studies have used output from Global Climate Models (GCMs), which typically have native spatial resolutions on the order of 150–200 km, to force a hydrologic model offline. A key issue faced by such studies is the need to translate inputs to a hydrology model, which operates at a higher spatial resolution than the GCMs. In the PNW, as in other topographically complex regions, it is necessary to reflect the effects of topographic barriers such as the Cascade Mountain range that control local climate. These issues have been addressed by downscaling techniques, most of which can also partly account for the bias inherent in GCM simulations, and convert precipitation (P) and temperature (T)
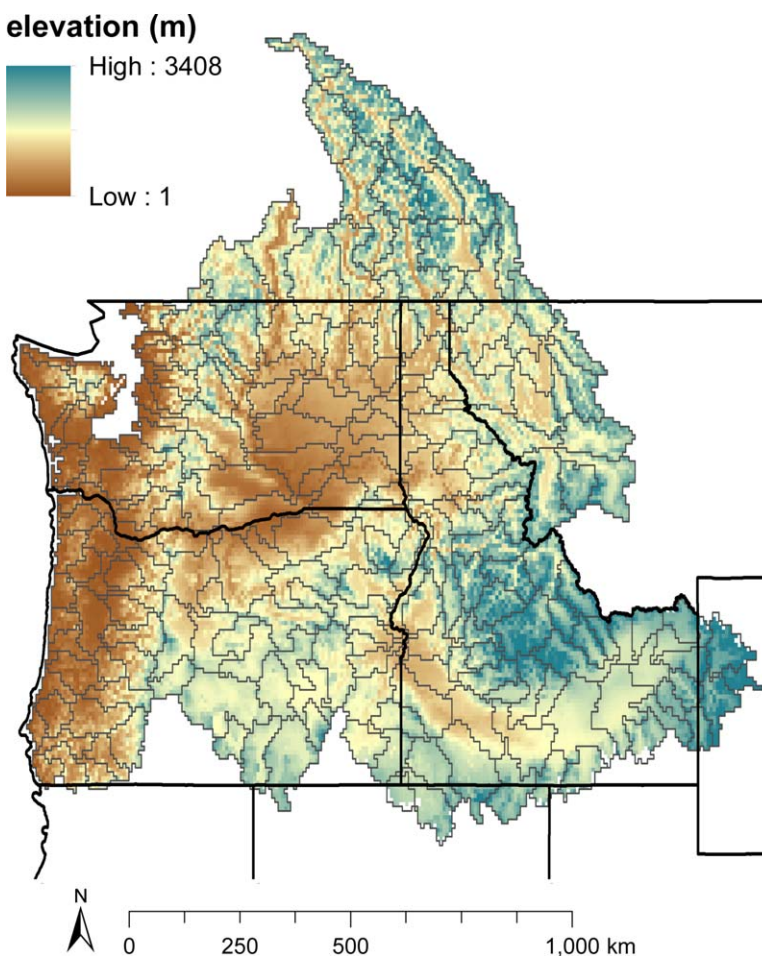
Figure 1. Pacific Northwest region including the Columbia River basin and coastal drainages. Elevation (which ranges from sea level to 4400 m) is shown as grid cell averages at 1/16° resolution. Watershed units, described in section 3.2, are outlined in gray.

changes from GCMs to local P and T using statistics from observation-based data sets [e.g., *Wood et al.*, 2004; *Abatzoglou and Brown*, 2012].

These studies are, however, resource intensive and subject to uncertainties related to the subset of GCMs used, the choice of hydrology model and the downscaling algorithm [*Vano et al.*, 2014]. In addition, it is challenging to determine whether differences associated with different GCM forcings are mostly due to changes in P or T and to distinguish the season in which these changes have the largest impact on basin-scale hydrologic predictions. This complicates the identification of regions that are more or less sensitive to future change [*Vano and Lettenmaier*, 2014].

We address the challenges of identifying locations and seasons that are most vulnerable to future change using an alternative, seasonal sensitivity-based, approach. We evaluate sensitivities to climate in terms of precipitation elasticity (ε), defined as the fractional change in runoff per fractional change in P, and temperature sensitivities (S), defined as the fractional change in runoff per °C change in T. In essence, we perform a sensitivity analysis of a hydrologic model, but instead of testing the sensitivity of model parameters, we evaluate the modeled response of changes in forcing variables P and T.

Previous studies have also quantified hydrologic sensitivities [*Schaake*, 1990; *Dooge*, 1992; *Dooge et al.*, 1999; *Sankarasubramanian et al.*, 2001; *Fu et al.*, 2007; *Vano et al.*, 2012, among others)]. *Dooge* [1992] derived an elegant approach that formulated the elasticities with respect to annual runoff of P and potential evapotranspiration. His approach is, however, complicated by the fact that potential evapotranspiration is not readily measurable in practice and in models is a derived quantity that involves a number of dependent variables. In contrast, surface air T is readily available for most GCMs, and is a metric most commonly

applied in climate change studies. Notably, temperature affects and is affected by hydrologic processes such as evaporation and snow processes. However, as cautioned by *Milly* [1992], temperature is not a static land-surface boundary condition, but rather is affected by latent heat exchange, something that is not accounted for in the off-line simulations investigated here. Other approaches motivated by a more complete set of sensitivities (e.g., net longwave radiation, potential evapotranspiration) could perhaps be explored, although we do not do so in this paper.

The seasonal sensitivity-based approach we outline is similar in concept to the approach used by *Vano et al.* [2012] in the Colorado River basin, where modeled sensitivities were evaluated at an annual time scale. In the PNW, however, a focus on the seasonal distribution of runoff and how it is impacted by seasonal changes in P and T is particularly important. Despite abundant annual P over much of the PNW, P occurs in the winter while water demand peaks in summer. The region's aggregate reservoir storage is much smaller than annual aggregate runoff, and reservoir storage is more distributed among multiple facilities than in the Colorado River basin. As such, modest changes in the seasonal distribution of runoff have the potential to affect reservoir system performance. Additionally, future climate projections in the PNW indicate that different seasons will experience greater changes than others [*Abatzoglou et al.*, 2014; *Mote et al.*, 2013] and therefore understanding the impact of seasonal changes (e.g., cool versus warm season warming) is valuable.

This study builds on the work of *Elsner et al.* [2010] and *Das et al.* [2011]. *Elsner et al.* [2010] classified PNW watersheds into rain-dominated, transitional, and snow-dominated based on the ratio of peak snow water equivalent (SWE) to accumulated winter (October to March) P. This classification scheme has been useful to water managers in the region and therefore has been included in subsequent user-funded studies [e.g., *Hamlet*, 2011; *Hamlet et al.*, 2013; *Tohver et al.*, 2014]. In this work, we also create a classification scheme to identify drivers of hydrologic change, but we base our analysis on modeled hydrologic sensitivities to P and T changes rather than results derived from GCM output. *Das et al.* [2011] evaluated warm versus cool season responses to T change in four major western U.S. river basins—the Colorado, Sacramento (North Sierra), San Joaquin (South Sierra), and Columbia—using the Variable Infiltration Capacity (VIC) model applied at 1/8° spatial resolution. They found that among these four large river basins, three are more sensitive to warming in the summer than in the winter, including the Columbia River. *Das et al.* [2011] did not, however, evaluate changes in the seasonality of runoff, but rather focused on the sensitivity of annual runoff changes to warm and cool season warming.

Our work is intended to provide a context for better understanding local-scale hydrologic change across the PNW by applying modeled hydrologic sensitivity concepts to map spatial variations in ε and S across the region (section 4.1). We categorize hydrologic sensitivities at the HUC-8 unit scale (average drainage area about 3000 km^2) (section 4.2) and evaluate modeled monthly response to seasonal changes in P and T (section 4.3). Finally, we evaluate the applicability of our monthly sensitivity construct to estimate future runoff changes (section 4.4) and provide examples for several tributaries (order 10^4-10^5 km^2). Although the method can be applied to any watershed, we focus on the Willamette River at Portland (Willamette), Yakima River near Parker (Yakima), Columbia River at Keenleyside Dam (Upper Columbia), the Snake River at Ice Harbor Dam (Snake), and the Columbia River at The Dalles (Dalles), subbasins that capture a diversity of responses and are important from a water management standpoint.

Throughout our comparisons, we consider the nature of modeled hydrologic sensitivities with an emphasis on two key properties, linearity and superposition. Linearity is used to evaluate the extent to which sensitivities based on a small change (e.g., 0.1°C) can provide a reasonable approximation of the sensitivity to a much larger change (e.g., 3°C). Note that the sensitivities are defined as a change in runoff per degree change in forcing. Divergence of the sensitivities to small and large T increases indicates nonlinearities in the hydrologic system. Superposition is the extent to which hydrologic sensitivities identified through independent perturbations of P and T can be added to approximate the effects of changes applied concurrently. Superposition properties determine whether changes applied in different seasons in independent simulations (e.g., a 0.1°C increase in October to March and a 0.1°C increase in April to September) can be added together to estimate the joint response (e.g., a 0.1°C annual increase). When both properties of linearity and superposition hold, the transfer functions we develop are most applicable.

2. Site Description

We define the Pacific Northwest (PNW) as the Columbia River basin and its adjacent coastal drainages (USGS Hydrologic Region 17 plus the Canadian portion of the Columbia). It is a diverse hydroclimatic region with varied vegetation, soil, and topography [*Stanford et al.*, 2005], with elevations ranging from sea level to 4400 m (Figure 1). Although hydrologic observations are somewhat sparse in the headwaters, climatic and streamflow data are generally sufficient to evaluate model predictions across most of the hydroclimatic conditions experienced in the region [*Elsner and Hamlet*, 2010].

The region's water resources are managed by municipal, county, state, provincial, and federal agencies, which make spatial information that spans political boundaries particularly valuable. For example, the Columbia's headwaters are in Canada, and the Canadian portion (15% of the basin's drainage area) accounts for over a third of the river's flow at the mouth on average [*U.S. Army Corps of Engineers (USACE) and Bonneville Power Administration (BPA)*, 2012]. Furthermore, the basin's two largest reservoirs are in Canada. Joint management of the system for flood control and hydropower is controlled by the Columbia River Treaty of 1964. As this paper is being written, the 2014/2024 Columbia River Treaty Review process is underway with discussion of how the system should be operated in the future [*USACE and BPA*, 2012]. Among the concerns is how and where future runoff patterns might change in response to a changing climate.

3. Methods

3.1. Models and Forcing Data Set

We performed a set of control experiments using the Variable Infiltration Capacity (VIC) macroscale land-surface hydrology model [*Liang et al.*, 1994]. We used VIC version 4.0.7 calibrated and validated as in *Hamlet et al.* [2010, chapter 5]. This implementation has a higher spatial resolution (1/16° versus 1/8°) and generally improved performance relative to earlier implementations [e.g., *Hamlet and Lettenmaier*, 1999; *Payne et al.*, 2004]. The increased spatial resolution improves the ability of the model to represent topographic effects and resolve smaller watersheds and hence provide information relevant to local water management concerns [*Elsner and Hamlet*, 2010; *Wenger et al.*, 2010].

We forced the VIC model using the same 1/16° latitude-longitude historical model forcing data set developed in previous efforts [*Elsner et al.*, 2010; *Hamlet et al.*, 2010]. The data set includes daily values of P, maximum and minimum air T, and wind speed, which are used in a preprocessing step based on the MTCLIM algorithms [*Thornton and Running*, 1999] to calculate other forcing variables such as longwave radiation, shortwave radiation, and relative humidity (for details see *Bohn et al.* [2013]). Note that the VIC model as implemented operates at a 1 h time step when snow is present, and daily otherwise. The MTCLIM algorithms produce hourly model forcings as necessary from the daily P and T max/min inputs. The model was cold started on 1 January 1915 and spun up for the period 1915–1970. The model state at the end of this period served as the initial state for all subsequent model experiments. We simulated P and T perturbations for the period 1970–2004 and calculated sensitivities over the reference period 1975–2004. Our choice of a relatively recent three-decade period reflects our desire to use a baseline period consistent with recent climate. However, past work has shown that hydrologic model sensitivities do not change much when calculated over different time periods [*Vano et al.*, 2014].

3.2. Hydrologic Sensitivities

We estimated hydrologic sensitivities, precipitation elasticity (ε), and temperature sensitivity (S), as defined in *Vano et al.* [2012]. We calculated ε and S using control experiments where a baseline simulation was compared with a simulation in which either P or T was perturbed. We used the VIC model because it has been well tested in the region and results from previous studies could be used in comparisons. The concept is, however, transferable and can be used with other hydrologic and land-surface models [e.g., *Vano et al.*, 2012]. For the computation of both ε and S, changes were applied for different time periods: year round (every day of the year), in the warm season (every day in April to September), in the cool season (every day in October to March), and in four 3 month seasons (every day in October to December, January to March, April to June, and July to September referred to as OND, JFM, AMJ, and JAS, respectively). Results were averaged over the 30 year reference period. We estimated ε and S using 1% P increases and 0.1°C increases. We also applied

3°C increases when determining watershed classifications, which corresponds to the T change projected by 16 GCMs in the latter part of the 21st century [*Das et al.*, 2011], for annual, warm season, and cool season perturbations. This 3°C increase allowed direct comparison with *Das et al.* [2011].

We examined the character of hydrologic sensitivities at three spatial scales (grid cell, watershed, and major subbasin). At the grid level (1/16° or approximately 30 km²), we calculated sensitivities for each of the 24,108 grid cells in our PNW domain. At the intermediate watershed scale, hydrologic quantities were aggregated over 226 watershed units (USGS HUC-8 cataloging units in the U.S. and GeoBase National Hydro Network Work Unit in Canada). The watershed units have an average drainage area of 3000 km² (ranging from 200 to 11,600 km²). We aggregated runoff from all 1/16° grid cells that lie at least 50% within these watershed boundaries. Finally, we calculated the aggregate sensitivities for the Willamette River, Yakima River, Snake River, Upper Columbia River, and Columbia River at The Dalles as noted in section 1. When calculating hydrologic sensitivities at the grid level or watershed scale, we simply aggregated the runoff values (sum of the model's surface runoff and drainage) over the area of interest. For the major subbasins, we used runoff values routed to a particular stream gage (streamflow) using the routing model of *Lohmann et al.* [1998] to account for channel travel times.

We developed two watershed classifications to emphasize differences in S across the region. The first classification is based on differences in the annual response (total magnitude) to warming applied in different seasons and includes three categories: (1) locations where annual S is more negative when warming is applied in the cool season rather than the warm season, (2) locations were the opposite is true, i.e., annual S is more negative when warming is applied in the warm season rather than the cool season, and (3) locations where warming applied in the cool season results in positive annual S values, which is a special case of category two. The second classification identifies locations that are sensitive to shifts in seasonality. Categories within this classification are based on the difference in S between the warm season and the cool season in response to cool season warming. Further details on these two classifications are provided in sections 4.2.3 and 4.2.4, respectively.

3.3. Estimating Future Streamflow

We used the following procedure to construct monthly future hydrographs from monthly ε and S values (employed as transfer functions) in response to seasonal P and T changes. Four sets of monthly ε and S were calculated by applying 1% P and 0.1°C T increases in OND, JFM, AMJ, and JAS (eight total VIC simulations) where values were relative to the historical simulation in each month. Regional-average, seasonal GCM changes (ΔP (%) and ΔT (°C)) in OND, JFM, AMJ, and JAS were also calculated between the historical period (1970–1999) and three future periods, 2020s, 2040s, and 2080s (defined as 2010–2029, 2030–2059, 2070–2099, respectively). Future monthly flows were then constructed based on equation (1)

$$Q_{fut}^i = Q_{his}^i \prod_{j=1}^{4} \left(1 + \varepsilon_j^i \Delta P_j\right)\left(1 + S_j^i \Delta T_j\right) \tag{1}$$

where *i* is the month (1–12, with month 1 corresponding to October), *j* is the season (1–4, with season 1 corresponding to OND), Q_{fut}^i is the future flow in month *i*, Q_{fut}^i is the historic flow in month *i*, ΔP_j and ΔT_j are changes in season *j*, and ε_j^i and S_j^i are the precipitation elasticity and temperature sensitivity, respectively, in month *i* in response to a change in season *j*. This equation captures the interaction terms as cross products. Further details are included in section 4.4.

We compare our seasonal sensitivity-based monthly hydrographs with hydrographs generated using the more involved full-simulation approach produced for 10 GCMs by *Hamlet et al.* [2010] (available online at http://warm.atmos.washington.edu/2860/products/sites) for the five major subbasins introduced in section 1. *Hamlet et al.* [2010] used the same hydrologic model, historical forcing data, and streamflow routing scheme as in this study. To generate "full-simulation" values, however, they also downscaled the GCMs using the hybrid delta method to get daily P and T output to run VIC, after which they routed the streamflow and bias corrected it (for all locations except the Willamette, where only streamflows without bias correction were available).

4. Results and Discussion

4.1. Spatial Variations in Hydrological Responses
4.1.1. Precipitation Elasticities (ε)
To determine the extent to which warm and cool season changes contribute to basin-wide sensitivities, we applied a 1% P increase year round (Figure 2, left column, top plot), in the warm season (middle), and in the cool season (bottom). As an example, an ε of 3 in the upper left plot of Figure 2 implies that a 1% increase in P applied throughout the year would result in a 3% increase in annual runoff. For 6 month changes, superposition holds: the lower two plots, which reflect the contribution of the warm and cool seasons to annual sensitivities, sum to the top plot to within ±0.15% for all grid cells (i.e., to a first approximation, warm and cool season ε values are additive). Seasonally applied P changes reflect the time of year when P is greatest. In other words, year-round ε is primarily determined by cool season changes (on average, more than 70% of the annual ε can be attributed to cool season changes), the season when the majority of P occurs in the PNW.

Precipitation elasticities (ε) exhibit seasonal responses that vary by location due to temperature (mostly related to snow processes). These seasonal responses are straightforward (and therefore not shown). When P change is applied in the warm season, essentially all runoff change occurs in the warm season. When P change is applied in the cool season, runoff changes occur in the cool season at low elevations and in the warm season at high elevations. However, overall, relative P increases in the cool season generate more runoff because cool season P is both more abundant and more efficient in producing runoff through a large spring pulse than warm season P.

4.1.2. Temperature Sensitivities (S)
The right column of Figure 2 shows the sensitivity of annual responses to warming applied annually, in the warm and in the cool season. Superposition applies in most grid cells. That is, the sum of the responses to warm and cool season warming is close to the response to year-round warming (within ±0.25% per °C for 94% of grid cells). Spatially, there is a range of responses including both increases (blue) and decreases (red) in annual runoff. If warming occurs only in the cool season, 74% of the grid cells show decreases in annual runoff, whereas if warming occurs throughout the year 93% of the grid cells show decreases in annual runoff. The larger number of cells with decreases results because declines from warm season warming are greater than increases from cool season warming for most grid cells.

The mechanism by which runoff increases in response to warming is sometimes referred to as the Dettinger hypothesis, described in *Jeton et al.* [1996]: due to warming, water leaves the system earlier in the year (as a result of earlier snowmelt or because P falls as
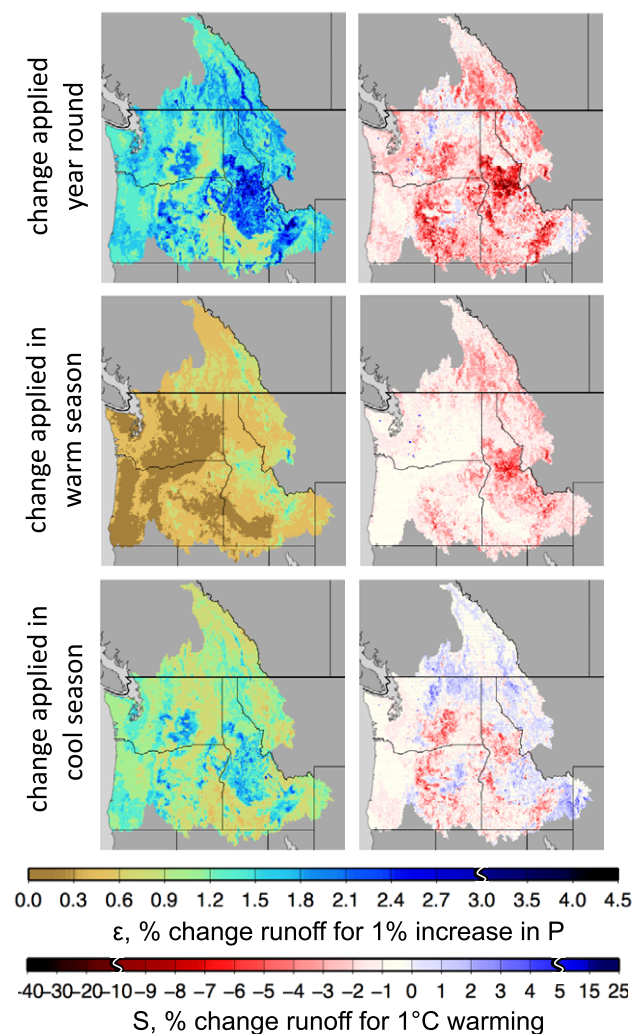

change applied year round

change applied in warm season

change applied in cool season

| 0.0 | 0.3 | 0.6 | 0.9 | 1.2 | 1.5 | 1.8 | 2.1 | 2.4 | 2.7 | 3.0 | 3.5 | 4.0 | 4.5 |

ε, % change runoff for 1% increase in P

-40-30-20-10-9 -8 -7 -6 -5 -4 -3 -2 -1 0 1 2 3 4 5 15 25

S, % change runoff for 1°C warming

Figure 2. Annual responses to (left) P (ε values) and (right) T (S values) change. Breaks in color bars indicate changes in increment.

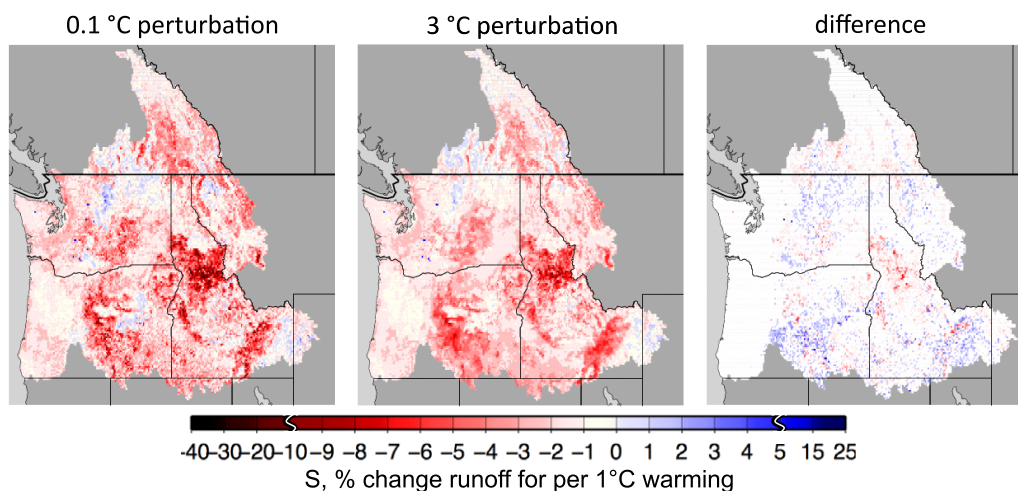**Figure 3.** Temperature linearity, effects of T increment on annual temperature sensitivities (S). S values (ranging from −16% to +15%) from simulations using a (left) 0.1°C increase and a (right) 3°C increase and differences between the two. Differences in S less than one are shown in white (right plot).

rain rather than snow) and is not available for evapotranspiration later in the year. Therefore, it is possible for runoff to be higher in a warmer climate, even without a change in P.

In aggregate, we found the annual response was greater from warming applied in the warm season than warming applied in the cool season, which is similar to *Das et al.* [2011] values at The Dalles, but local watershed-level responses varied (discussed in section 4.2.2). Note that *Das et al.* [2011] evaluated the basin response to a 3°C increase. This response differs from an empirical analysis by *Berghuijs et al.* [2014] of 97 small U.S. catchments that showed greater streamflow declines from temperature changes in November to March than in May to September, highlighting an area where more mechanistic work would be helpful.

To test the effect of the different change increment, and hence the linearity of annual S values, we compared the patterns of annual S values across the PNW using a 0.1°C increment with those generated using a 3°C increment (Figure 3). The patterns are similar and differences between a 0.1°C and 3°C perturbation are less than 1% in 78% of the grid cells (and less than 2% in 95% of grid cells). Sensitivities calculated with the smaller perturbation (0.1°C) are generally greater in absolute value (both larger increases and decreases in runoff) than those calculated with the 3°C perturbation. While larger T changes have the potential to melt more snow, this snow may not be available. In the case that all the snowmelts for a T increase of less than 3°C, the sensitivities in response to a 3°C perturbation are smaller than those for a 0.1°C (note that all sensitivities are expressed per °C warming).

Figure 4 shows how warming imposed annually and in each season (rows) contributes to changes in individual seasons, where the left column is the annual response (same three plots as in Figure 2), the middle column is the change in the warm season, and right column is the change in the cool season. Values are calculated relative to annual runoff. Therefore, by definition, the warm and cool season S add to the annual S (horizontally, denominators are the same). Warm season warming reduces runoff throughout the year, whereas cool season warming increases runoff in the cool season but reduces runoff in the warm season. Therefore, although the net runoff change is less for warming in the cool season than in the warm season, the change in seasonality is much greater for cool season warming. The differences in hydrologic responses in warm and cool seasons are largely controlled by regions at higher elevations (identified in Figure 1). This is particularly important as not all seasons show equal warming [*Abatzoglou et al.*, 2014]. Future projections of seasonal change in the PNW indicate greater warming in the summer than other seasons [*Mote et al.*, 2013].

4.2. Categorizing Hydrologic Changes at the Watershed Scale
4.2.1. Annual Watershed-Level Precipitation Elasticities (ε) and Temperature Sensitivities (S)
We complement the fine-scale spatial information in Figures 2 and 4 with watershed-level categorizations. Figure 5 shows the watershed-scale response to annual P and T changes. This information is similar to the top plots in Figure 2, but is averaged for each of the 226 watersheds in the region. Watershed annual ε
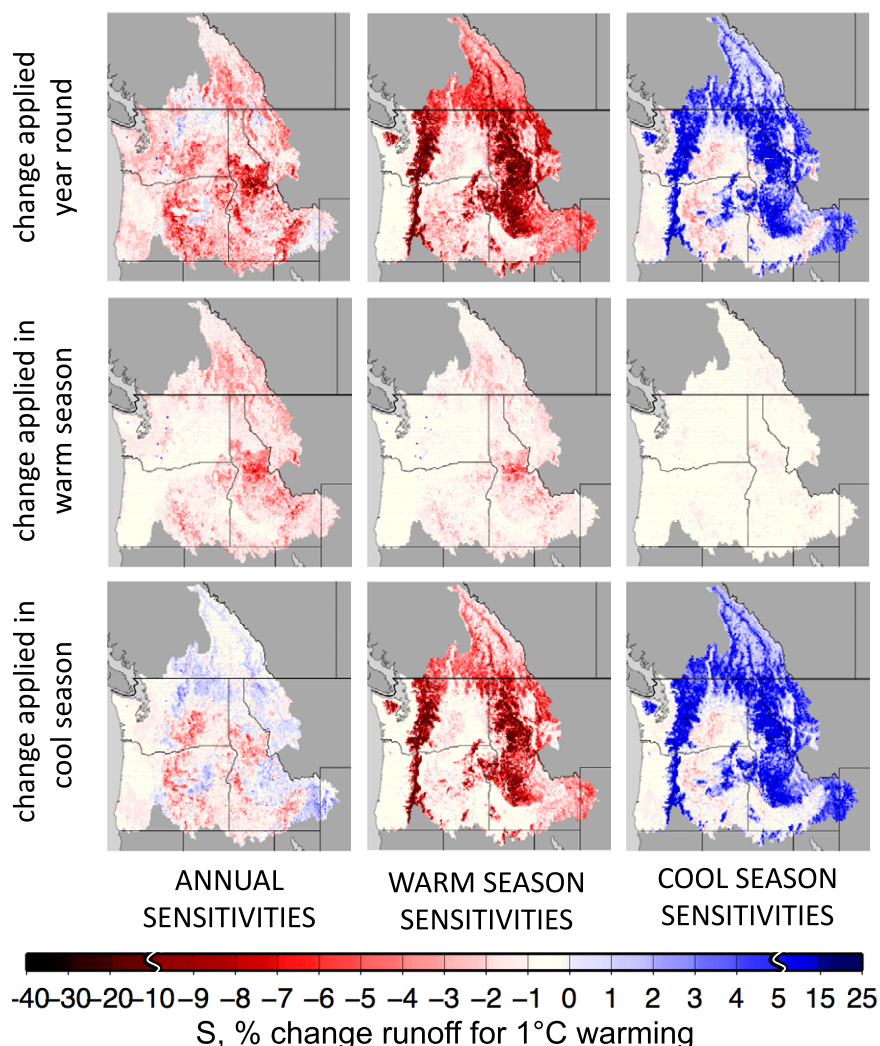
Figure 4. Seasonal responses to warming. (left) Annual sensitivities (% change in annual runoff per °C warming) and the contribution of that change in the (center) warm season and (right) cool season for warming applied throughout (top) the year; (middle) only in the warm season; and (bottom) only in the cool season. The annual sensitivities (left plots) contain the same information as annual sensitivity values in Figure 2. The breaks in the color bar indicate a change in increments, emphasizing the larger absolute values of warm and cool season sensitivities.

values range from 0.9 to 2.5. Five watersheds have an ε of less than one. These locations have low annual P and are located at lower elevations in eastern Washington and the Middle Snake subbasin. Watersheds with higher ε values are located in west-central Idaho in midelevation to high-elevation regions where model simulations show relatively low runoff ratios. These annual values can be compared with results from *Sankarasubramanian et al.* [2001] who evaluated precipitation elasticities from annual P and streamflow observations throughout the conterminous U.S. using a nonparametric observation-based estimator of elasticity. Within the PNW, the map provided in *Sankarasubramanian et al.* [2001] has contours with magnitudes ranging from 1.0 to 2.0, with a similar increase in elasticities from west to east, although they report higher values in eastern Oregon, rather than west-central Idaho. Their continental-scale analysis is at a coarser spatial resolution than ours (dictated by station locations), which may explain why specific locations do not align.

Regions with the greatest annual S values in response to annually applied T changes (Figure 5, right) are also clustered in the upper Salmon River basin of central Idaho, while less sensitive areas are at both extremes of the elevation spectrum—low lying coastal areas (rain-dominated watersheds) and headwaters in Canada and Wyoming (snow-dominated watersheds). All watersheds show decreases in runoff with increasing T (S values range from −0.2% to −8% per °C), i.e., increases in runoff represented by the blue grids in Figure 4 top left, are outweighed by decreases when averaged with the other grids in the
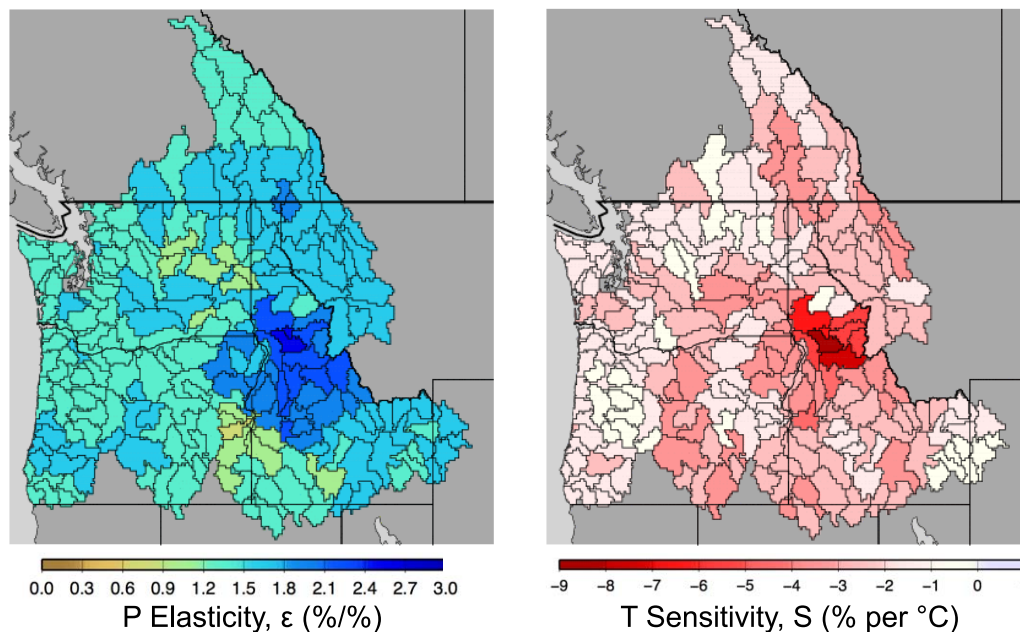
P Elasticity, ε (%/%)   T Sensitivity, S (% per °C)

Figure 5. Watershed-scale annual precipitation elasticities (ε) and temperature sensitivities (S). Annual responses (percent) to annually applied change (percent precipitation change or °C warming).

watershed. These *annual responses* to *annually applied changes* capture one aspect of S. In the next section, we discuss characterizations that address seasonality.

4.2.2. Annual Responses to Warm and Cool Season Warming (Total Magnitude)

Figure 6a classifies the 226 watersheds into one of three categories according to the annual sensitivity to warm and cool season warming (using a 3°C change increment):

1. *More Sensitive to Cool Season Warming*. Locations where annual runoff declines more with cool season warming than with warm season warming. 83 of the 226 subbasins (36%), mostly low elevation watersheds, have this characteristic, which is similar to temperature sensitivities in the southern Sierra shown in *Das et al.* [2011].

2. *More Sensitive to Warm Season Warming*. Annual runoff magnitudes decline more with warm season warming than with cool season warming. This characteristic is seen in basin-wide responses in the Colorado, Columbia, and North Sierra [*Das et al.*, 2011]. This response is most common (in 64% of watersheds, including the special case below), occurring for watersheds at midelevation and high elevation and at higher latitudes along the coast.

3. *Cool Season Warming Positive*. In this special case, warming applied in the cool season generates increases in cool season runoff that are greater than decreases in warm season runoff resulting in net increases in runoff (i.e., warmer winter temperatures lead to increased annual flows). This occurs in 14% of watersheds in the PNW (Figure 6a), most of which are at high elevations (see Figure 1 for elevations).

In general, even though the Columbia River basin as a whole has substantially greater sensitivity of annual runoff to warm rather than cool season warming (category 2), 27% of the 151 watersheds upstream of The Dalles show the reverse behavior, being more sensitive to cool season warming (category 1). These basins are mostly at lower elevations in Oregon, eastern Washington, and southern Idaho. This pattern pertains to many of the coastal drainages downstream of The Dalles as well, especially in Oregon (Figure 6a, yellow watersheds).

4.2.3. Seasonal Responses to Warming (Shifts in Seasonality)

To quantify the sensitivity of watersheds to shifts in seasonality, we defined six categories that are gradations of the difference between cool season and warm season sensitivities to cool season warming
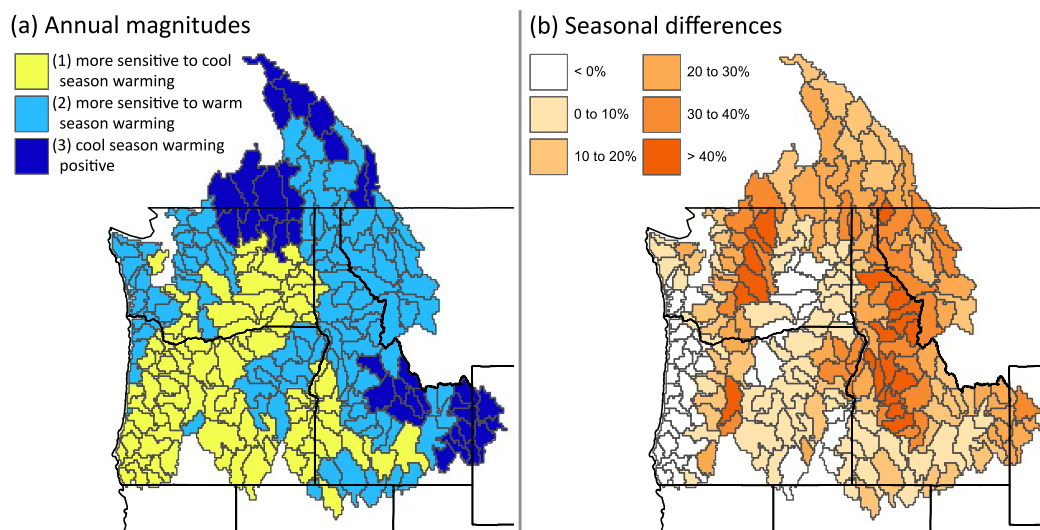
Figure 6. PNW watershed classifications. (a) Watershed classifications based on temperature sensitivities to warm and cool season warming of 3°C that reflect the time of year having the greatest impact on annual flow magnitudes; (b) classifications based on difference in percentage points between warm and cool season S when warming is applied in the cool season. Larger differences (dark orange) are more likely to experience seasonal differences in their hydrographs as temperatures increase.

for all PNW watersheds (Figure 6b). These differences are similar to differences in percentage points between the middle and right columns of Figure 4 for change applied in the cool season. Watersheds having the largest differences (dark orange) are watersheds most sensitive to warming since, in this region, the difference is largely due to runoff increasing in the cool season and subsequently decreasing in the warm season. These dark orange watersheds correspond to watersheds that change from snow-dominated to mixed snow/rain systems in future simulations as seen in *Elsner et al*. [2010] and *Tohver et al*., [2014]. In other words, watersheds that change from one regime (e.g., snow-dominated) to another (e.g., transient) are also those that exhibit the greatest seasonal shifts in runoff (largest differences) in response to cool season T perturbations. Both snow-dominated, high-elevation watersheds (hydrographs peak in the spring), as well as rain-dominated, low-elevation watersheds (hydrographs peak in the fall-winter) do not show large differences in their warm and cool season S. For these basins, warming does not result in a regime change because they remain cold enough that the applied warming does not affect the timing of their snowmelt, or because they are already rain dominated and so there is little snow to melt.

4.3. Monthly Responses to Seasonal Precipitation and Temperature Changes

To quantify monthly responses, we applied changes in 3-month periods (OND, JFM, AMJ, and JAS), calculated monthly responses (supporting information Tables A1 and A2), and created "bubble" diagrams (Figure 7) similar to those in *Nijssen et al*. [2001]. These bubble diagrams show how changes applied in one season (*y* axis) effect changes in streamflow in every month of the year (*x* axis, starting in October) for five major subbasins.

Figure 7 shows ε_j^i and S_{j}^i, where *j* is the season in which the change is applied (*y* axis) and *i* is the month in which the resulting streamflow change is evaluated (*x* axis; also see equation (1)). For example, ε_2^{12} is the elasticity of September streamflow in response to a 1% change in P imposed during the JFM season. Values across the top row (marked "ALL") are calculated from simulations where the change is applied in every month of the year whereas the individual rows are based on simulations in which changes are imposed in an individual season. In general, superposition holds, meaning changes are additive, i.e., the sum of the four 3-month rows equals the "ALL" row, but for reasons discussed below, this is not always the case. The rightmost column (marked "Y") shows the annual change, which is the total difference throughout the year divided by the annual streamflow (note: values do not add horizontally as they are percentages for individual months, i.e., denominators differ).

Precipitation elasticity values (Figure 7, middle) for four of the basins (all except the Willamette) are similar because P changes applied in OND, JFM, and AMJ all affect streamflow response throughout the summer. This
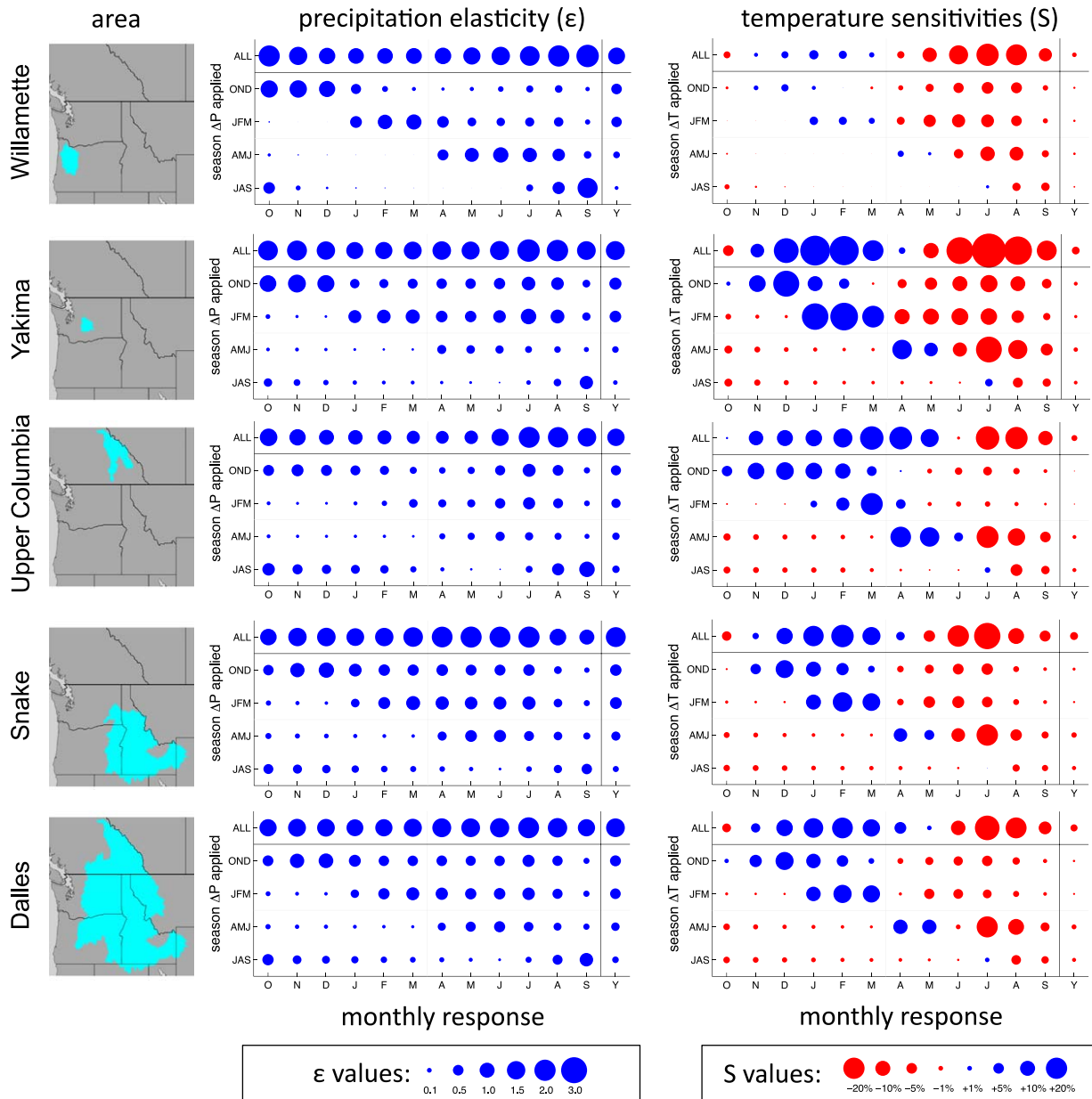
Figure 7. Monthly responses to seasonal P (ε, % change streamflow per % change P) and T changes (S, % change streamflow per °C). Warming is applied in 3-month periods (OND, JFM, AMJ, JAS) and throughout the year (ALL), and responses (ε or S) are shown for each individual month relative to that month (O, N, D, . . . S) as well as the annual response (Y). Maps on the left show the contributing area for each tributary.

reflects the nature of large tributaries in the Columbia River basin. All are snowmelt dominated (see historical hydrographs in Figure 10), illustrating the dependence of the seasonal P response on seasonal T (as discussed in section 4.1.1). Only rain-dominated basins, typically located on the west side of the Cascades, have monthly ε values where the majority of the streamflow changes occur in the same months as the P perturbation. The Willamette, which has a greater peak from rain in the fall and winter than from snowmelt in the spring, is an example of a basin where responses are smaller (because of less snow) and correspond more directly with the timing of P changes.

The bubble diagrams for S (Figure 7, right) show how streamflow responses to warming vary by basin. The larger blue (increases) and red (decreases) bubbles highlight basins that are most sensitive to change (e.g., Yakima) and the time of year when S transitions from positive to negative. For example, the largest bubbles
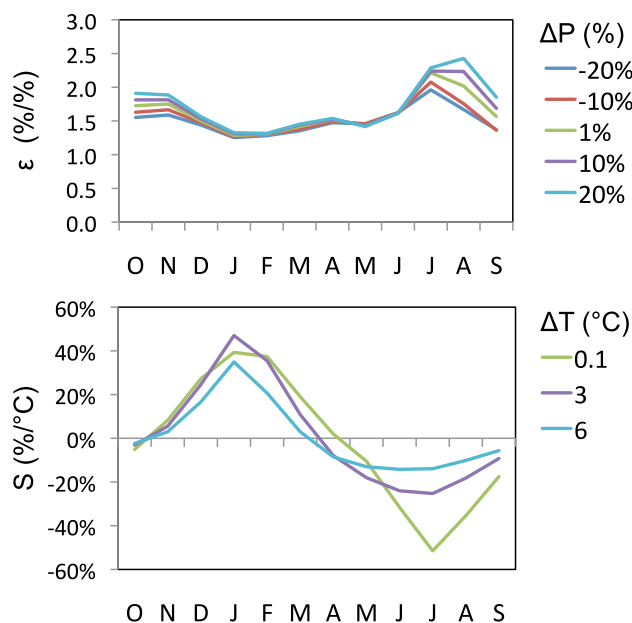
Figure 8. Monthly responses for (top) precipitation elasticities, ε, and (bottom) temperature sensitivities, S, in the Yakima River basin calculated using different change increments (colored lines). The largest differences (greatest nonlinearities) occur in the summer time, when lines diverge.

in the Willamette (red bubbles in JJA on the x axis) indicate decreases in summer streamflow in response to warming in all seasons, while winter streamflow is relatively insensitive to warming (blue bubbles from November to March are small relative to other basins). Note that the bubble diagrams show changes relative to each month so the absolute changes in winter may still be larger than in summer. The Yakima, Upper Columbia, and Snake are all currently snow dominated, but the Yakima is more vulnerable to T increases in JFM than the other basins and, based on this analysis, could experience a greater change in seasonality as T increases. The Upper Columbia and Snake are more affected by AMJ warming (see AMJ row relative to others) as higher elevations (hence lower T) provide a buffer such that these basins are relatively insensitive to winter warming. The Dalles reflects the combined basin response, but the domain is essentially overweighted by the areas contributing the most runoff; hence, this domain is most similar to the high-elevation headwater tributaries.

4.3.1. Linearity of Monthly Responses to Seasonal Change

We test the linearity of monthly responses by varying the increment of annually applied change used to calculate ε and S values in the Yakima (Figure 8). If the response were linear, ε and S values would be the same (note that ε and S are normalized to represent the change in streamflow for +1% P or +1°C T, respectively). For ε values, we applied increments of −20%, −10%, +0.1%, +10%, and +20%. For this range of increments, winter and spring responses are approximately linear, while summer and fall responses are not (the largest range in seasonal ε values is in August, which coincides with low flows). For S values, we applied increments of +0.1, +3, and +6°C. Again, streamflow responds similarly during certain months regardless of the increment (e.g., October and November), but considerable differences exist, especially in the summer. The large differences in the summer correspond to the time of year when streamflow is historically low, and relatively small changes in magnitude can have a large effect on ε and S.

4.3.2. Superposition of Monthly Responses to Seasonal Change

For P changes, superposition generally applies, that is, monthly ε values are close to additive (supporting information Table A1). Values of ε for each of the four 3-month periods (the OND, JFM, AMJ, JAS rows) calculated with a 1% P change in those seasons, closely sum to ε values calculated from a 1% P change applied annually (the ALL row). The absolute difference is less than 1% for all but 1 month at one location. The Yakima in September shows a larger difference (−4.7%), which corresponds to the lowest flow month when small absolute changes result in larger relative changes.

For T changes, superposition holds less uniformly. Annual S values for seasonally applied T changes are generally additive, whereas monthly S values for seasonally applied T changes, especially for large T increments, are not (supporting information Tables A2 and A3). For example, in the Yakima, the annual S value calculated based on a 0.1°C increase in temperature applied year round is nearly identical to the annual S value calculated as the sum of the responses to a 0.1°C increase applied in each of the four seasons separately (−2.667% versus −2.672% per °C, respectively) (supporting information Table A2). Similarly, annual S values

calculated in these two ways based on a 3°C increase differ by only 0.37% per °C (supporting information Table A3).

In contrast, whether monthly S values adhere to principles of superposition depends on the increment of change. In the Yakima, monthly S values calculated with a +0.1°C change are still mostly additive: the sum of the four seasons is only 1.7% per °C lower in August and 1.6% per °C higher in September than monthly S values calculated from annually applied T change (supporting information Table A2). Alternatively, monthly S values calculated with an increment of +3°C range from the sum of the four seasons being 18.2% points lower in July (−43.5% versus −25.3%) to 13.5% points higher in April (+5.6% versus −7.9%) (supporting information Table A3). Differences in monthly S values become even greater if changes are applied in individual months instead of 3-month intervals (not shown). This nonadditive response can be attributed to the influence of snowpack and the fact that T increases, if applied in individual seasons and then added together, can effectively "melt the same snow twice," resulting in estimates of higher spring-time and lower summertime streamflow. This highlights the importance of selecting change increments that approximate the tangent of the change function when superposition will be applied (as in section 4.4). Of the five locations simulated, the Yakima has the largest change in seasonal streamflow with T increases, and thus is most sensitive to these T effects.

4.4. Application to Climate Change Projections

A practical application of the seasonal hydrologic sensitivities outlined above is to use monthly ε and S values in response to seasonal change as transfer functions to convert seasonal changes in P and T from GCMs into future projections of monthly hydrographs. Although the method is approximate and only provides an estimate of changes in the mean monthly streamflow (and not, for instance, changes in variability or a multiyear time series), it has the advantage that it is much less time consuming than full-simulation methods. In this section, we illustrate how the seasonal sensitivity-based method compares with the full-simulation method of *Hamlet et al.* [2010].

Seasonal sensitivity-based hydrographs were calculated by applying P and T changes from GCM simulations for each 3-month season (equation (1), see supporting information and equation (A1) for an alternative form of the equation). For the Yakima, we evaluated how our results were affected by the inclusion (equation (1)) or exclusion (equation (A2) in supporting information) of the interaction terms (Table 1). The interaction terms represent the compounded effects of changes in P and T in one season on the runoff in other seasons, for example $S^1_{OND}\Delta T_{OND}S^1_{JFM}\Delta T_{JFM}$. The Yakima basin has the greatest seasonal sensitivity to warming of the five basins and would be most sensitive to this change. We found that including seasonal interaction terms is most important for T changes in this basin. If P interactions are not included, results change only slightly. If future seasonal P and T changes were applied without interaction terms (supporting information equation (A2)), *annual responses* are closest to full-simulation results, but the seasonal sensitivity-based hydrographs significantly overestimate reductions in summertime streamflow compared to full-simulation hydrographs. For example, streamflow becomes negative in the Yakima in July for some scenarios in 2040 and all scenarios in 2080 (Table 1). The inclusion of the interaction terms reduces summertime declines by applying the change fractions to values that have been reduced according to T impacts in other seasons. In the same way, wintertime streamflow can be inflated. Nonetheless, negative streamflow values can result as changes are being applied in a linear manner when, in reality, sensitivities are nonlinear. For example, if there is a 4°C increase in AMJ when July's sensitivity is −29% per °C, the percent decline will be over 100%. Consequently, this estimation method works best for small changes (e.g., more typically ∼30 years into the future rather than 100) and for basins with modest sensitivities, where nonlinearities in the sensitivities are small. Overall, this method is useful only for the seasonal nature of hydrograph changes rather than the absolute magnitude of future streamflow. The latter, either annually or in a particular season, should be viewed with caution.

Figure 9 and Table 1 show results for the Yakima for three future time periods. Generally, the seasonal sensitivity-based method reproduces the change in seasonality quite well, providing similar information about both the average seasonal response (average of the 10 GCMs) and ensemble range, even as climate change becomes more pronounced in 2080. This method best captures the near-term changes, which are also of greater importance to water managers for ∼30 year planning horizons. As expected, the ensembles (gray lines) of the seasonal sensitivity-based method are smoother than those from the full-simulation

Table 1. Yakima Scenarios, Differences From Historical Streamflow

	2020	2040	2080
% Difference in Annual Magnitudes			
Full-simulation [*Hamlet et al.*, 2010]	*2% (−11 to 15%)*	*5% (−15 to 22%)*	*6% (−12 to 31%)*
P and T interactions (Figure. 8 and 9)	−0% (−14 to 18%)	5% (−6 to 24%)	14% (−12 to 47%)
No interactions	−1% (−16 to 16%)	2% (−10 to 19%)	5% (−21 to 30%)
T interactions only	−0% (−15 to 17%)	5% (−6 to 23%)	14% (−13 to 45%)
% Increases in Winter (November to April)			
Full-simulation [*Hamlet et al.*, 2010]	*30% (5 to 53%)*	*48% (28 to 87%)*	*72% (39 to 127%)*
P and T interactions (Figures 8 and 9)	22% (2 to 55%)	44% (27 to 82%)	83% (39 to 153%)
No interactions	22% (4 to 50%)	43% (29 to 71%)	79% (49 to 122%)
T interactions only	22% (2 to 55%)	44% (27 to 81%)	83% (38 to 149%)
% Decrease in Peak Flow (May)			
Full-simulation [*Hamlet et al.*, 2010]	*−13% (−21 to 2%)*	*−25% (−55 to 1%)*	*−51% (−79 to −1%)*
P and T interactions (Figures 8 and 9)	−9% (−20 to 1%)	−16% (−26 to 4%)	−35% (−64 to 0%)
No interactions	−8% (−21 to 1%)	−12% (−22 to 6%)	−26% (−53 to 7%)
T interactions only	−10% (−20 to 1%)	−16% (−26 to 4%)	−35% (−64 to 1%)
% Decrease in Low Flow (July)			
Full-simulation [*Hamlet et al.*, 2010]	*−45% (−63 to −30%)*	*−63% (−86 to −43%)*	*−84% (−94 to −68%)*
P and T interactions (Figures 8 and 9)	−49% (−69 to −30%)	−71% (−94 to −41%)	−97% (−112 to −77%)
No interactions	−57% (−89 to −30%)	−89% (−142 to −37%)	−157% (−257 to −86%)
T interactions only	−50% (−69 to −30%)	−71% (−94 to −41%)	−157% (−257 to −86%)

[a]Transfer functions were applied to seasonal values of P and T changes for each GCM. Differences are between historical streamflows (1970–1999) and three future periods (2010–2029, 2030–2059, 2070–2099). Values are the average and range of 10 GCMs for the A1B emissions scenario, the same ones simulated by *Hamlet et al.* [2010], also shown in this table.
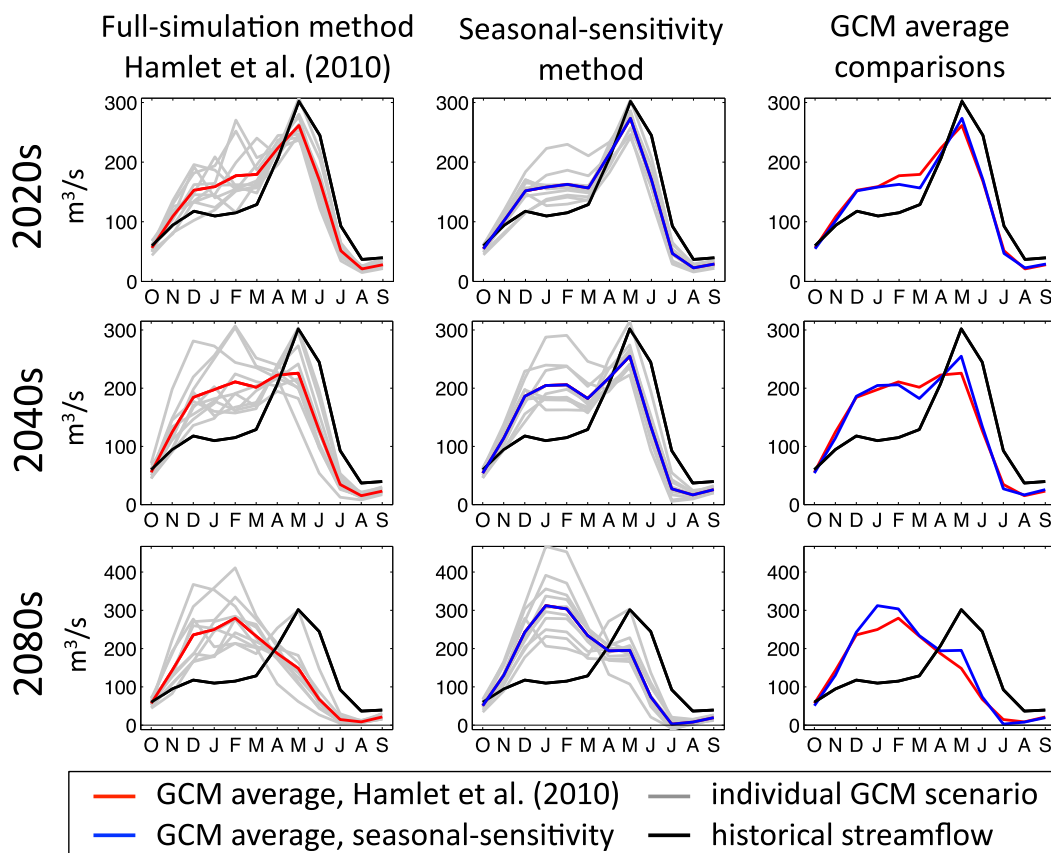

Figure 9. Yakima River basin at Parker monthly average streamflow projections for the 2020s, 2040s, and 2080s for the A1B emissions scenario. The left plots are results from *Hamlet et al.* [2010], which use a full-simulation method, whereas the middle plots are generated using the seasonal sensitivity-based method presented in this study. The right plots compare averages of the 10 GCMs for both methods.
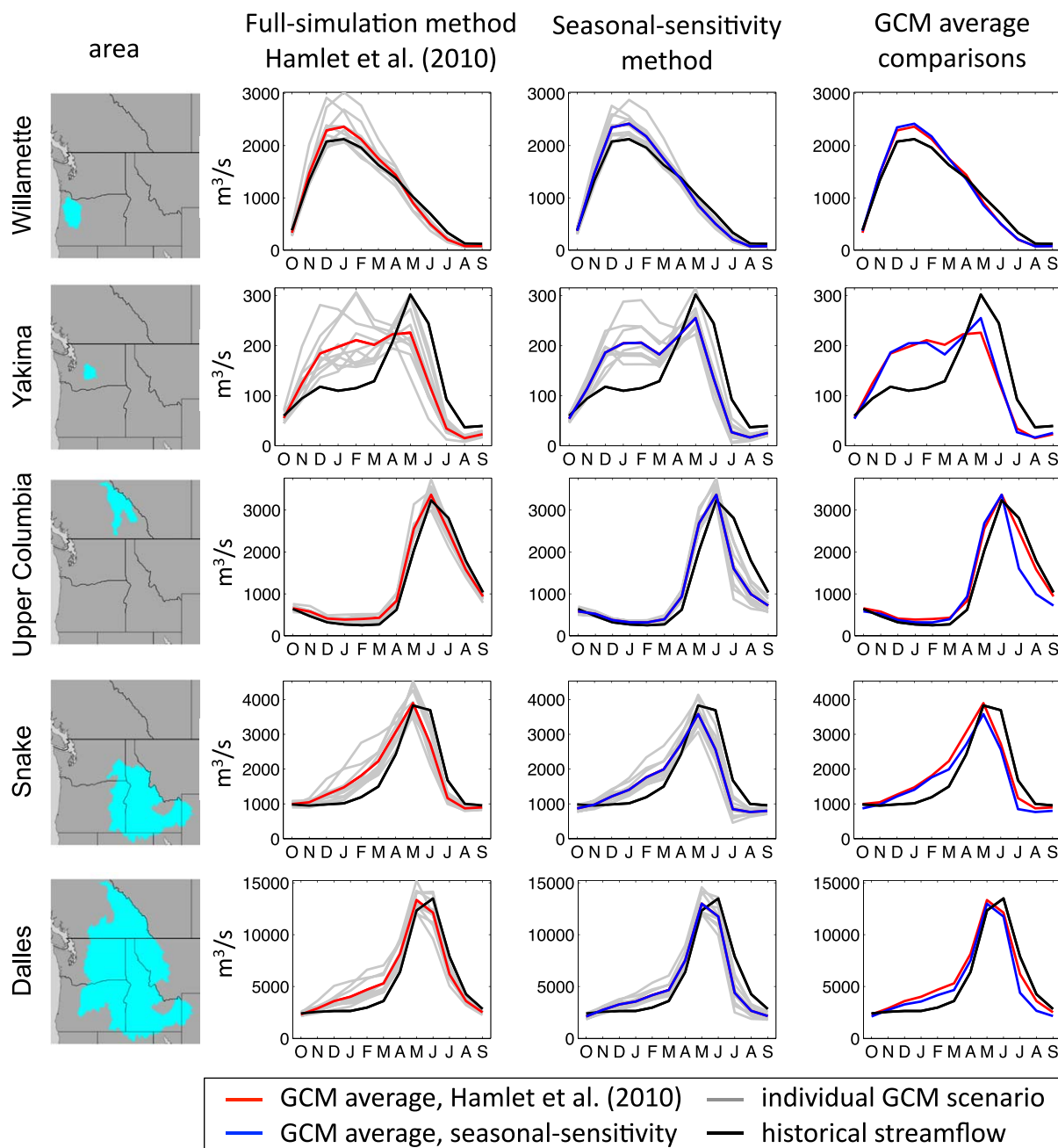
Figure 10. Comparison of monthly average streamflow projections similar to Figure 9 but for only the 2040s at five locations throughout the Columbia River basin.

method, since they are based on changes applied to long-term averages. For summertime streamflow, the seasonal sensitivity-based method captures the nature of the changes, but actual magnitudes are not realistic for reasons mentioned earlier.

We compare results between these two methods in five locations (Figure 10), across the spectrum of rain-dominated (Willamette) to snow-dominated basins (Upper Columbia), as indicated by the season of peak streamflow. We present results from 2040 as it tests the method more than 2020, but is not as extreme as 2080, and provides more information for near-term water management planning. Results show that across the spectrum, the seasonal sensitivity-based method captures the nature of seasonal changes, both in the average and range of seasonal responses. The greatest difference between the two methods is the rate at which streamflow declines between June and September. This relates to

the nonlinearity in the seasonal response, which is greater in the summer (as highlighted in Figure 8). Additionally, the seasonal sensitivity-based approach is most vulnerable to error when S values are large and negative, which also occurs in the summer (especially in July). In all cases, and especially in locations with the coldest temperatures (e.g., Upper Columbia), the seasonal sensitivity-based stream-flow declines faster than that of the full-simulation streamflow. In the bubble diagram for the Upper Columbia, this is seen as the contrast between the positive S in June and the large negative S in July; when change is continuous, as in the full-simulation, this transition is less abrupt. Overall, summertime streamflow with the seasonal sensitivity-based method is lower (a more conservative estimate) than with the full-simulation method.

In general, these results support a straightforward approach to estimating changes in monthly streamflow based on future changes in monthly P and T from GCMs. The approach uses only two sets of 48 values each (12 monthly values times 4 seasons), one for ε and one for S, as transfer functions to reproduce seasonal changes created from detailed model simulations. This simplified approach provides plausible monthly hydrographs, but has important limitations. Its utility and accuracy are greater for applications of seasonal shifts, not changes in total magnitude. This study has focused on seasonal shifts because water manage-ment in the PNW is more concerned with climate-forced seasonalities (due to small reservoir capacity rela-tive to annual streamflows) than with total magnitude changes. If, however, magnitudes are more important, the alternate sensitivity-based technique that emphasizes adjustments designed to capture annual responses [*Vano and Lettenmaier*, 2014] may be more appropriate. Another limitation is that the set of ε and S values presented here are specific to the baseline T and current land cover in the historical hydro-logic model simulations. If these change then the sensitivities will likely also change. Changing T and land cover are less of a problem in the near term and are also not reflected in most full-simulation approaches. Updating ε and S values would require nine model runs, which is a considerably less demanding computa-tional effort than that required for full-simulation estimations (number of GCMs $\times$ number of emission sce-narios $\times$ number of future time periods). Generally, the seasonal sensitivity-based method described and tested here uses linear approximation of seasonal ε and S, which in fact are nonlinear. This typically results in overestimates of streamflow changes, especially in summer, and an exaggeration of the transition from the cool to the warm season.

5. Conclusions

The Pacific Northwest (PNW) will show different responses to climate change depending on the specific location, season, and magnitude of P and T change. To better define how the region, and its local water-sheds, will respond to future change, we map the sensitivities of runoff to modeled changes in P and T both spatially and temporally. We use concepts of hydrologic sensitivities to (a) quantify watershed classifi-cations that help define local hydrologic changes and (b) develop a methodology where sensitivities serve as a transfer function that can be used to quickly convert average seasonal P and T changes into an esti-mate of future hydrographs for local watersheds.

Through application of the hydrologic sensitivity approach to the PNW we found:

1. Transitional (intermediate elevation) watersheds experience the greatest seasonal shifts in runoff in response to cool season warming.

2. For watersheds that receive much of their winter P as snow (i.e., snow-dominated and transitional water-sheds), warming applied in the cool season, results in both greater change in the seasonality of runoff and smaller reductions in annual runoff compared to warming applied in the warm season.

3. The net change from cool season warming results in annual runoff increases for 26% and decreases for 74% of the domain. Runoff increases occur in the high-elevation regions in primarily snow-dominated watersheds but are overwhelmed by decreases when averaged over larger areas or when warming is also applied in the warm season.

When applying hydrologic sensitivities to future change, we found:

1. The ability to construct hydrographs from monthly hydrologic sensitivities depends on how well hydro-logic sensitivities adhere to principles of linearity and superposition. For this reason, the seasonal sensitivity-based method works best for modest changes (e.g., ∼30 years into the future rather than 100,

which is also a more typical planning horizon for management agencies) and for basins where sensitivities are modest, hence nonlinearities in the sensitivities are small.

2. Seasonal P changes (and their monthly ε values calculated using an increment of 1%) are largely independent of each other (e.g., the runoff response from P increases in JFM and AMJ generally have minimal interaction), adhering to principles of superposition.

3. Seasonal T changes (and their monthly S values calculated using a $+0.1°C$ increment) also appear to be additive, although less so than for P. We found 3-month seasonal T changes based on a $+0.1°C$ increment resulted in largely independent responses. However, if the increment of change is larger (i.e., $+3°C$), superposition does not hold. In the case of $+3°C$, the simple approach can essentially double count the response by melting the same snow twice.

4. Future changes in T should be incorporated using an approach that accounts for interactions between seasons. This results in estimated future hydrographs that more closely replicate hydrographs generated using the full-simulation approach. Conversely, interactions between seasons for P changes have little effect on the estimated future hydrograph.

5. The seasonal sensitivity-based method compares well with the full-simulation method in these basins for purposes of capturing the nature of changes in seasonality. There are, however, seasons and locations where P and T changes are more nonlinear; and caution should be used in interpreting the absolute streamflow magnitude (rather than the relative change), especially in the summer and when future T increases are large.

References

Abatzoglou, J. T., and T. J. Brown (2012), A comparison of statistical downscaling methods suited for wildfire applications, *Int. J. Climatol.*, *32*, 772–780, doi:10.1002/joc.2312.

Abatzoglou, J. T., D. E. Rupp, and P. W. Mote (2014), Understanding seasonal climate variability and change in the Pacific Northwest of the United States, *J. Clim.*, *27*, 2125–2142, doi:10.1175/JCLI-D-13-00218.1.

Berghuijs, W. R., R. A. Woods, and M. Hrachowitz (2014), A precipitation shift from snow towards rain leads to a decrease in streamflow, *Nat. Clim. Change*, *4*(7), 583–586.

Bohn, T. J., B. Livneh, J. W. Oyler, S. W. Running, B. Nijssen, and D. P. Lettenmaier (2013), Global evaluation of MTCLIM and related algorithms for forcing of ecological and hydrological models, *Agric. For. Meteorol.*, *176*, 38–49, doi:10.1016/j.agrformet.2013.03.003.

Das, T., D. W. Pierce, D. R. Cayan, J. A. Vano, and D. P. Lettenmaier (2011), The importance of warm season warming to western U.S. streamflow changes, *Geophys. Res. Lett.*, *38*, L23403, doi:10.1029/2011GL049660.

Dooge, J. C., M. Bruen, and B. Parmentier (1999), A simple model for estimating the sensitivity of runoff to long-term changes in precipitation without a change in vegetation, *Adv. Water Resour.*, *23*, 153–163, doi:10.1016/S0309-1708(99)00019-6.

Dooge, J. C. I. (1992), Sensitivity of runoff to climate change: A Hortonian approach, *Bull. Am. Meteorol. Soc.*, *73*, 2013–2024.

Elsner, M. M., and A. F. Hamlet (2010), Macro-scale hydrologic model implementation, report, University of Washington, Seattle, Wash. [Available at http://warm.atmos.washington.edu/2860/r7climate/study_report/CBCCSP_chap5_vic_final.pdf.].

Elsner, M. M., L. Cuo, N. Voisin, J. S. Deems, A. F. Hamlet, J. A. Vano, K. E. B. Mickelson, S. Y. Lee, and D. P. Lettenmaier (2010), Implications of 21st century climate change for the hydrology of Washington State Climatic Change, *Clim. Change*, *102*(1), 225–260.

Federal Columbia River Power System (FCRPS) (2001), *The Columbia River System Inside Story: Federal Columbia River Power System*, 2nd ed., Bonneville Power Admin., Portland, Oreg.

Fu, G., S. P. Charles, and F. H. S. Chiew (2007), A two-parameter climate elasticity of streamflow index to assess climate change effects on annual streamflow, *Water Resour. Res.*, *43*, W11419, doi:10.1029/2007WR005890.

Hamlet, A. F. (2011), Assessing water resources adaptive capacity to climate change impacts in the Pacific Northwest Region of North America, *Hydrol. Earth Syst. Sci.*, *15*(5), 1427–1443.

Hamlet, A. F., and D. P. Lettenmaier (1999), Effects of climate change on hydrology and water resources in the Columbia River basin, *J. Am. Water Resour. Assoc.*, *35*(6), 1597–1623.

Hamlet, A. F., et al. (2010), Final project report for the Columbia Basin climate change scenarios project, report, University of Washington, Seattle, WA. [Available at http://www.hydro.washington.edu/2860/report/.].

Hamlet, A. F., M. M. Elsner, G. S. Mauger, S. Y. Lee, I. Tohver, and R. A. Norheim (2013), An overview of the Columbia basin climate change scenarios project: Approach, methods, and summary of key results, *Atmos. Ocean*, *51*(4), 392–415, doi:10.1080/07055900.2013.819555.

Jeton, A. E., M. D. Dettinger, and J. L. Smith (1996), Potential effects of climate change on streamflow, eastern and western slopes of the Sierra Nevada, California and Nevada, *U.S. Geol. Surv. Water Resour. Invest. Rep.*, 95–4260, 44 pp.

Lee, S. Y., A. F. Hamlet, C. J. Fitzgerald, and S. J. Burges (2009), Optimized flood control in the Columbia river basin for a global warming scenario, *J. Water Resour. Plann. Manage.*, *135*(6) 440–450, doi:10.1061/(ASCE)0733-9496(2009).

Liang, X., D. P. Lettenmaier, E. F. Wood, and S. J. Burges (1994), A simple hydrologically based model of land surface water and energy fluxes for general circulation models, *J. Geophys. Res.*, *99*, 14,415–14,428.

Lohmann, D., E. Raschke, B. Nijssen, and D. P. Lettenmaier (1998), Regional scale hydrology: I. Formulation of the VIC-2L model coupled to a routing model, *Hydrol. Sci. J.*, *43*(1), 131–141.

Luce, C. H., and Z. A. Holden (2009), Declining annual streamflow distributions in the Pacific Northwest United States, 1948–2006, *Geophys. Res. Lett.*, *36*, L16401, doi:10.1029/2009GL039407.

Luce, C. H., J. T. Abatzoglou, and Z. A. Holden (2013), The missing mountain water: Slower westerlies decrease orographic enhancement in the Pacific Northwest USA, *Science*, *342*(6164), 1360–1364.

Mantua, N., I. Tohver, and A. F. Hamlet (2010), Climate change impacts on streamflow extremes and summertime stream temperature and their possible consequences for freshwater salmon habitat in Washington State, *Clim. Change*, *102*(1–2), 187–223, doi:10.1007/s10584-010-9845-2.

Milly, P. C. D. (1992), Potential evaporation and soil moisture in general circulation models, *J. Clim.*, *5*(3), 209–226.

Mote, P., J. Abatzoglou, and K. Kunkel (2013), Climate change in the Northwest, in *Climate Change in the Northwest: Implications for Our Landscapes, Waters, and Communities*, edited by M. Dalton, P. W. Mote, and A. K. Snover, chap. 2, 224 pp., Island Press, Washington D. C.

Nijssen, B., G. M. O'Donnell, A. F. Hamlet, and D. P. Lettenmaier (2001), Hydrologic sensitivity of global rivers to climate change, *Clim. Change*, *50*(1), 143–175.

Payne, J. T., A. W. Wood, A. F. Hamlet, R. N. Palmer, and D. P. Lettenmaier (2004), Mitigating the effects of climate change on the water resources of the Columbia River basin, *Clim. Change*, *62*, 233–256.

Safeeq, M., G. E. Grant, S. L. Lewis, M. G. Kramer, and B. Staab (2014), A hydrogeologic framework for characterizing summer streamflow sensitivity to climate warming in the Pacific Northwest, USA, *Hydrol. Earth Syst. Sci.*, *18*(9), 3693–3710.

Sankarasubramanian, A., R. M. Vogel, and J. F. Limbrunner (2001), Climate elasticity of streamflow in the United States, *Water Resour. Res.*, *37*, 1771–1781.

Schaake, J. C. (1990), From climate to flow, in *Climate Change and U.S. Water Resources*, edited by P. E. Waggoner, pp. 177–206, John Wiley, N. Y.

Stanford, J. A., F. R. Hauer, S. V. Gregory, and E. B. Snyder (2005), The Columbia River, in *Rivers of North America*, edited by A. C. Benke and C. E. Cushing, Elsevier, Boston, Mass.

Thornton, P. E., and S. W. Running (1999), An improved algorithm for estimating incident daily solar radiation from measurements of temperature, humidity, and precipitation, *Agric. For. Meteorol.*, *93*, 211–228.

Tohver, I. M., A. F. Hamlet, and S.Y. Lee (2014), Impacts of 21st-Century Climate Change on Hydrologic Extremes in the Pacific Northwest Region of North America. *J. of the American Water Resour. Assoc. 50*(6), 1461–1476, doi: 10.1111/jawr.12199.

U.S. Army Corps of Engineers (USACE) and Bonneville Power Administration (BPA) (2012), Columbia River Treaty, Portland, Oreg. [Available at http://www.crt2014-2024review.gov/, last accessed 15 June 2012.]

Vano, J. A., and D. P. Lettenmaier (2014), A sensitivity-based approach to evaluating future changes in Colorado River Discharge, *Clim. Change*, *122*(4), 621–634, doi:10.1007/s10584-013-1023-x.

Vano, J. A., M. Scott, N. Voisin, C. O. Stockle, A. F. Hamlet, K. E. B. Mickelson, M. M. Elsner, and D. P. Lettenmaier (2010), Climate change impacts on water management and irrigated agriculture in the Yakima River basin, Washington, USA, *Clim. Change*, *102*(1–2), 287–317, doi:10.1007/s10584-010-9856-z.

Vano, J. A., T. Das, and D. P. Lettenmaier (2012), Hydrologic sensitivities of Colorado River runoff to changes in precipitation and temperature, *J. Hydrometeorol.*, *13*, 932–949, doi:10.1175/JHM-D-11-069.1.

Vano, J. A., et al. (2014), Understanding uncertainties in future Colorado River streamflow, *Bull. Am. Meteorol. Soc.*, *95*, 59–78, doi:10.1175/BAMS-D-12-00228.1.

Wenger, S. J., C. H. Luce, A. F. Hamlet, D. J. Isaak, and H. M. Neville (2010), Macroscale hydrologic modeling of ecologically relevant flow metrics, *Water Resour. Res.*, *46*, W09513, doi:10.1029/2009WR008839.

Wood, A. W., R. L. Leung, V. Sridhar, and D. P. Lettenmaier (2004), Hydrologic implications of dynamical and statistical approaches to downscaling climate model outputs, *Clim. Change*, *62*(1), 189–216, doi:10.1023/B:CLIM.0000013685.99609.9e.